COATING

Modeling of coating structure development

GUNER EKSI AND DOUGLAS W. BOUSFIELD

ABSTRACT

A three-dimensional model, based on pigment and binder size distributions, is proposed here to characterize coating structure development during consolidation. Particles are placed into a structure to simulate the dewatering event after coating. Coat weight, percent solid, particle populations, and sizes are the input variables of the model. The model predicts the physical position of spherical particles with any size distribution. From the knowledge of the physical positions of all particles, the void fraction, pore sizes, and roughness of the coating layer are obtained. Shrinkage and roughening are calculated when the latex particles coalesce into a film. Gloss is estimated from the roughness using literature relationships and the locations of different sized particles in the structure are obtained. The model gives porosity values for uniform spheres and bimodal distributions. Results indicate a nonuniform distribution of small particles in the structure. The model predicts that shrinkage and roughness increase with binder content. Pore size distribution calculations compare well with literature results, and details of the pore space are now characterized.

Application:

The model allows paper coaters to estimate the physical properties of a coating based on the pigment and latex size distributions.

PAPER COATINGS ARE APPLIED AS aqueous suspensions at high speeds. After the aqueous phase is removed by drainage into the sheet, a three-dimensional structure forms. Upon drying, latex particles deform causing the structure to shrink. Pigment-binder shape and size distributions are among the most important factors affecting this structure. The characteristics of the structural arrangement, the manner in which pigment particles are packed, and the distribution of binder and air spaces around them determine many properties of a coated paper such as gloss, opacity, porosity, roughness, pick resistance, and ink receptivity.

To develop new coating or paint formulations, much of current practice in industry is "trial and error." Different combinations of kaolin, calcium carbonate, titanium dioxide or other pigments are mixed with latex and other binders or additives to produce a trial coating. This trial coating is tested with hand drawdowns, high-speed laboratory coaters, and pilot trials for the desired optical, physical, and printing properties. However, these trials are costly and time consuming. Often little insight is gained as to why one combination does better than another. There exist now a number of relationships between structural parameters and optical properties, but there is no model to predict the structural parameters. A mathematical model is needed to help interpret experimental data and to predict the results of certain combinations of particles. A model, even with a number of approximations, should help reduce the need for many different trials. A model of this nature may be of use in many other industrial situations, such as filtration, papermaking, and ink setting.

The packing problem has been the subject of research for many industries and some studies have been made in this field. Because of its simple geometry, spheres have been used in most theoretical and practical studies on particle packing. The packing behavior of nonspherical particles is an empirical area and cannot be predicted theoretically at present. There are two different types of packing structures defined for monosized spheres: systematic and random. A systematic packing has a periodic structure that repeats over a specific distance. Graton and Fraser *(1)* gave the first description to the systematic approach of sphere packs. A random packing is constructed by a sequence of events that are not correlated with one another. Random packings of the particles are also arranged in two groups which are random loose and random dense packings, respectively. Real packed systems are usually random. A detailed description on packing of particles can be found in the literature *(2, 3)*.

The study of particle packing is based on the assumption that the particles are dense and discrete, they have a well defined size, often given in terms of an equivalent spherical diameter, and there are no particle-particle interactions between them. Computer simulations of random packing of spheres have been made by many scientists *(4-9)*. Initially similar techniques of model construction were employed in all techniques, such as adding each new sphere to the existing cluster at the site closest to the cluster center.

The model developed here is unique from other particle packing models in that particles are placed in such a manner as to simulate the

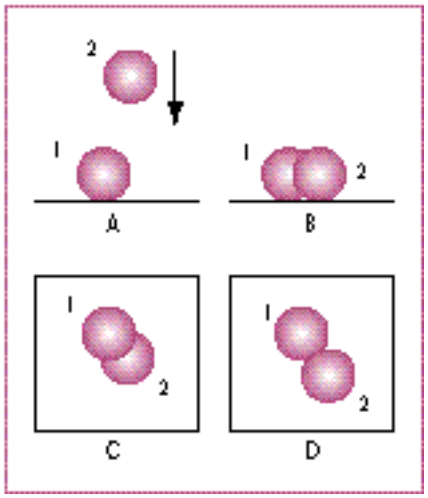

1. Illustration of the first case. Initial and final positions are shown. Particle 2 is moving; particle 1 is stationary. A: Front view, initial position. B: Front view, final position. C: Top view, initial position. D: Top view, final position.

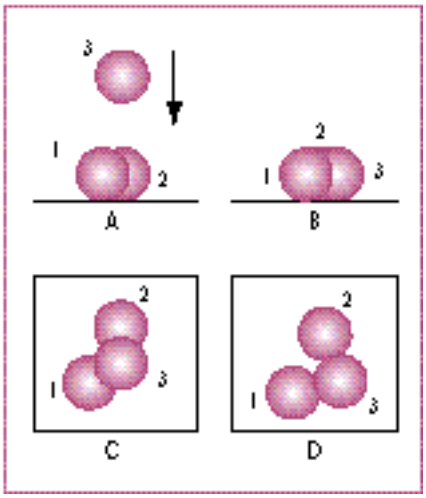

2. Illustration of the second case. Initial and final positions are shown. Particle 3 is moving; particles 1 and 2 are stationary. A: Front view, initial position. B: Front view, final position. C: Top view, initial position. D: Top view, final position.

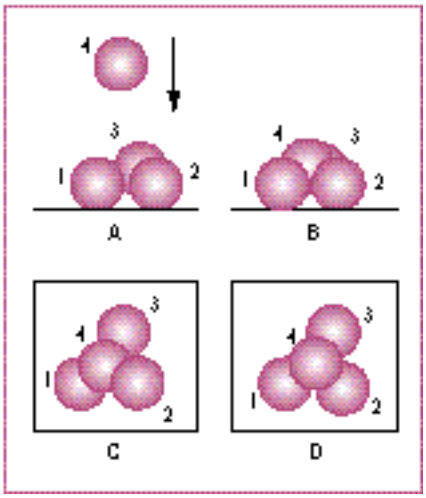

3. Illustration of third case. Initial and final positions are shown. Particle 4 is moving; particles 1, 2, and 3 are stationary. A: Front view, initial position. B: Front view, final position. C: Top view, initial position. D: Top view, final position.

dewatering of a coating to form a three-dimensional model: particles are moved downward into a structure because of fluid flow into the base paper. Only enough particles are used to describe thin coating layers. Full three-dimensional particles and structures are calculated. The porosity, size segregation, roughness, and shrinkage of the final structure are of interest. The model represents a novel approach to mathematically characterize the coating layer.

Experimental packing of monosized spheres gives void fractions between 0.359 and 0.43 *(10–13)*. Lee *(14)* and Van Gilder *et al. (15)* gathered experimental data from the literature on the packing of monosized spheres. From these data, they calculated average values for loose and dense random packing and concluded that the most-likely average void volume fractions of the loose and dense random packing of uniform spheres for infinite container-particle ratios are 0.411 and 0.361, respectively, in the absence of any particle-particle interactions, air-film effect, and external forces except gravitational force and mechanical shaking or vibration. Studies of packing of spheres with different size ratios between the particles have been reported *(12, 16, 17)*. The packing fraction of mixtures of spheres is greater than that of monosized spheres. The packing of mixtures of spheres is a function of the diameter ratios and volume compositions of the particles in the mixture.

The packing of pigment particles and the distribution of binder and air spaces around them affect the properties of the coating *(14, 15, 18–24, 32)*. Even though particle packing is very important for coated papers, there are limited theoretical studies *(14, 22, 23)* done with regard to paper coatings. Most theoretical work has dealt with empirical methods to predict maximum packing and viscosity, but there have been no calculations for the deposition of particles into thin layers. The literature details can be found in Eksi *(26)*.

The model predicts the physical position of all particles in a unit cell. From these positions, the porosity and roughness of the structure are calculated. This first state should approximate the first critical concentration (FCC) of Watanabe and LePoutre *(25)*. When the film forming spheres are allowed to "flow" and the particles are replaced, the porosity and roughness of the second critical concentration (SCC) are obtained along with the shrinkage. Details of the pore structure and the particle size distribution in the coating layer are calculated. The net result is the mathematical characterization of the coating layer before and after drying. The model is unique in that it is based on the physical situation after the blade.

MODEL DERIVATION

The model predicts the physical position of particles in a coating layer. The particles are placed in a three-dimensional structure in such a way as to simulate the dewatering event. The packing assumes that the non-hydrodynamic particle-particle interactions are larger than the hydrodynamic or lubrication interactions between particles. Therefore, calculations are based on geometric considerations. A number of other assumptions need to be made in a model of this type. The paper surface is assumed to be flat with no preferred regions of drainage. Drainage is assumed to be more rapid than drying. The particles are taken to be individual particles not in small

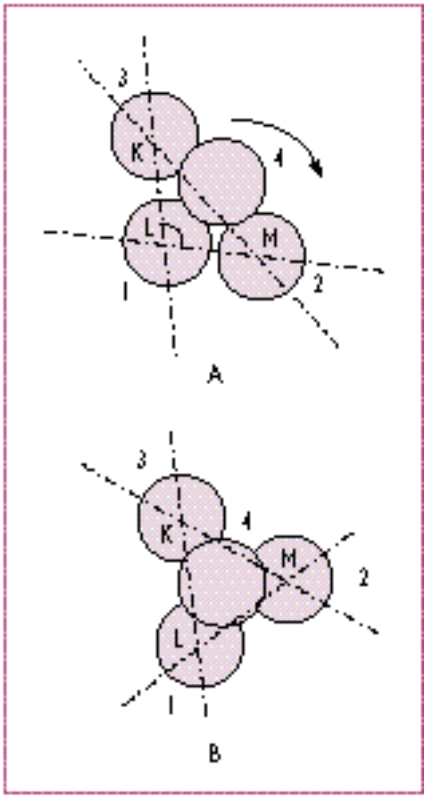

4. Illustration of the third case, top view for rolling (A) and non-rolling (B). If centers of particles 1, 2, and 3 are connected to each other, they make triangle KLM. If the center of the fourth particle is in the triangle, it does not roll as in (B).

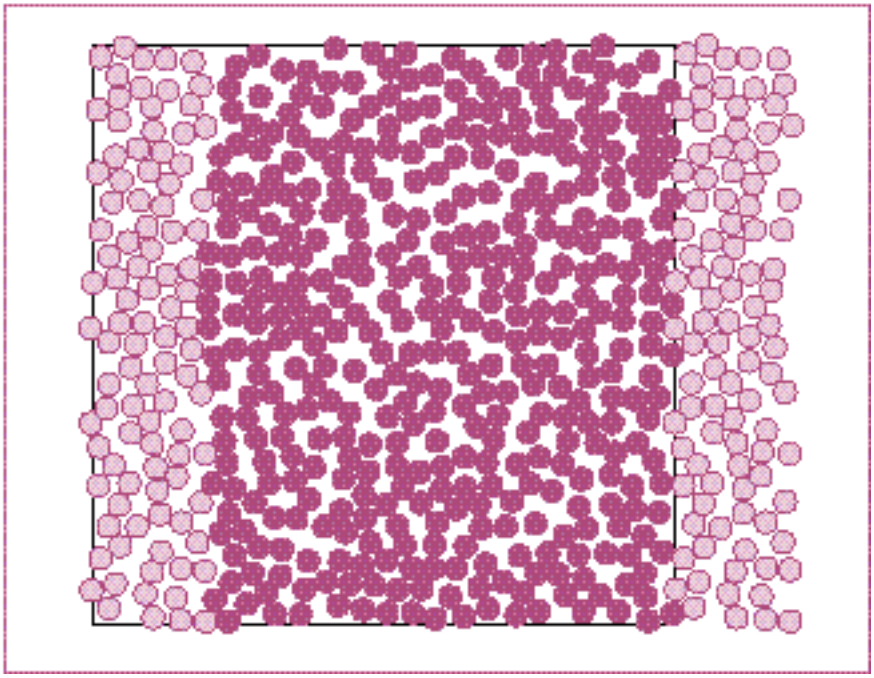

5. Top view of periodic boundary conditions. When placing a particle near the right hand boundary, a number of already placed particles are temporarily shifted to this boundary. The particle is placed under the influence of these shifted particles.

flocs. Once a particle is placed, it does not move because of other particles contacting it. At this time, all particles are taken to be spherical. However, this assumption can be relaxed in the future as this model technique is developed. The bottom surface is assumed to be flat even after contact with water. Again, this assumption can be relaxed in the future. Even with these assumptions, the model should be useful in understanding the ideal case. The details of the model derivation are in Eksi *(26)*.

Toivakka *et. al (27, 28)* give results for pigment motion during drying. The hydrodynamic forces are included in the calculations. However, these results are limited to uniform spheres in a monolayer. To understand the influence of different sized particles on the process, a three-dimensional model is needed. Here we present a three-dimensional model of a similar situation, but hydrodynamic forces between particles are neglected. A steady downward drag force on the particles is in mind as the particles are being placed.

PLACEMENT OF THE PARTICLES

Particles are introduced at random positions in a 3-D structure. The data file for the model includes the volume of the structure which is defined by the wet coating thickness, the length and the width of the structure, total number of particles, the number of different sized particles, and the radii of the particles. Random numbers are obtained from a standard random number generator *(29)*. Each particle, starting with the lowest particle, is moved downward as if dewatering is taking place. In the final structure, each particle touches at least three particles already in the structure. Each particle is supported by at least at three points.

Before placing a particle, the number of particles in its shadow that have already been placed in the structure is checked. One particle that is going to be placed sees other particles already placed in the volume. If there is no particle underneath the particle to be placed, final x and y positions of that particle are the same as its initial positions. Its z position is equal to its radius. If other particles are below, those particles are determined, and the particle is placed by solving the appropriate equations. These equations are in Eksi *(26)*. There are three different situations that can occur as a particle is placed in a structure. These situations relate to the number of particles the moving particle sees as it is moved downwards. **Figure 1** shows the first case where there is one particle below the particle to be placed. The second particle rolls off along the line connecting the centers of the particles. Its new x and y positions are calculated. Its new z position is equal to its radius if it is on the bottom layer. If this is not the bottom layer, the particle is placed with its new x and y positions on

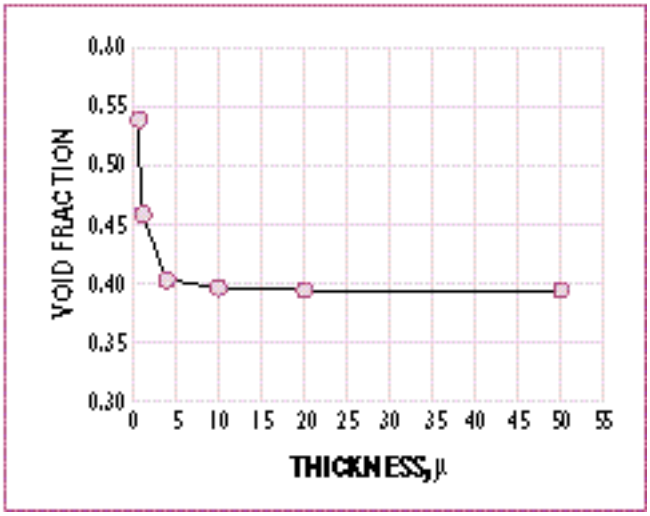

6. Void fraction is shown as a function of thickness. Monosized 0.25-μ radius particles have been used.

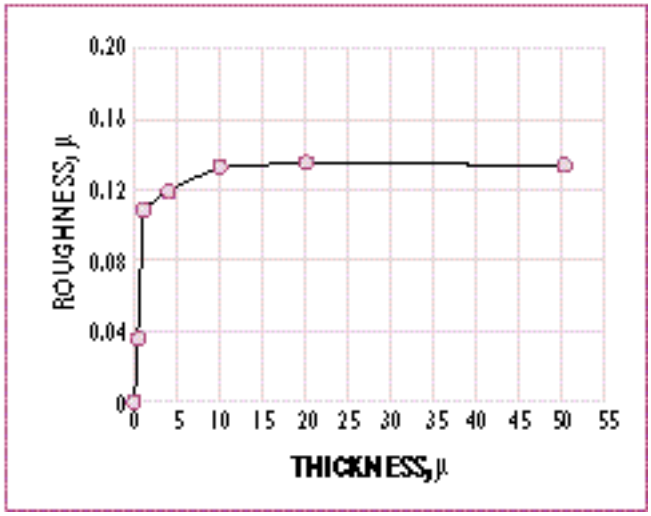

7. Roughness is shown as a function of thickness. Monosized particles having a radius of 0.25 μ have been used.

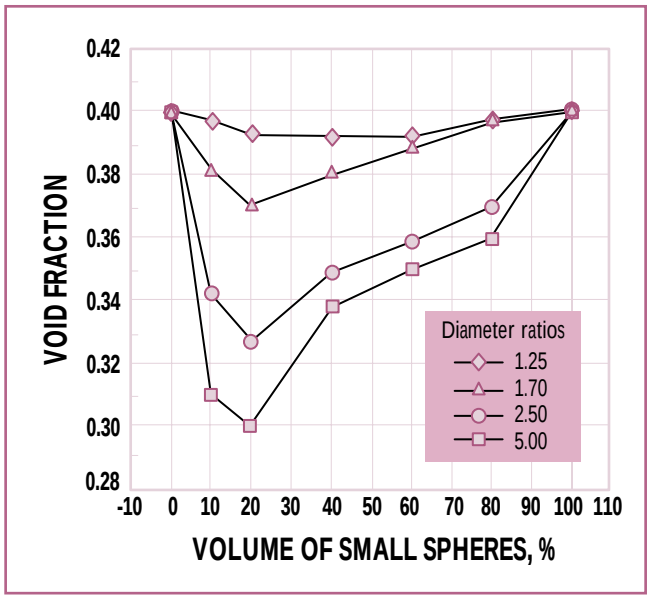

8. Porosity of binary mixtures of spheres as a function of percent volume of small spheres with diameter ratios of 1.25, 1.7, 2.5, and 5.0. The radius of the large spheres is 0.25 μ and the wet coating thickness is 10.0 μ.

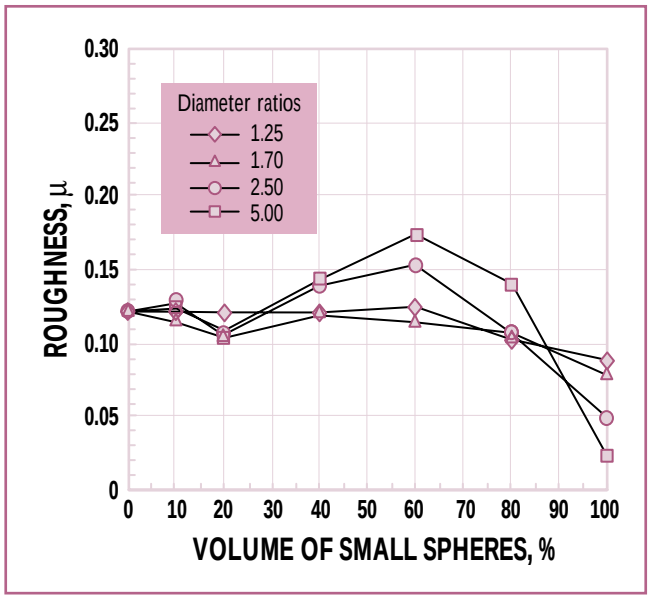

9. Roughness of binary mixtures as a function of percent volume of small spheres. Same parameters as in Fig. 8.

particles below it. In the second case, there are two particles just below the particle to be placed as seen in **Fig. 2**. The third particle rolls off and settles between the first and second particles. **Figure 3** shows the third case where the fourth particle is placed on top of the three particles, and its new *x, y,* and *z* positions are calculated. A Newton-Raphson technique is used to calculate the new *x, y,* and *z* positions. This placed particle is checked for rolling, as described later. Once the first layer is placed, this case is always the final case used to place the particles.

Checking for rolling

For every particle placed as in the third case, the possibility of the particle rolling to a lower position is checked. As fluid moves into the paper pore structure, three contact points with other particles are not enough to prevent further motion of the particle. The three contact points must support the "center of gravity" of the placed particle.

Figure 4 shows an illustration of the third case from the top view and how the rolling checking works. In Fig. 4, the lines connecting the centers of the particles 1, 2, and 3 make

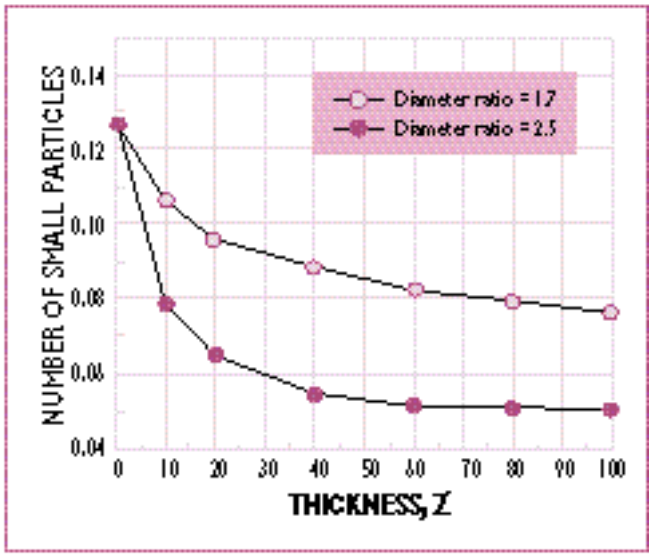

10. Average pore radius is shown as a function of the percent volume of small spheres. Diameter ratio is a parameter.

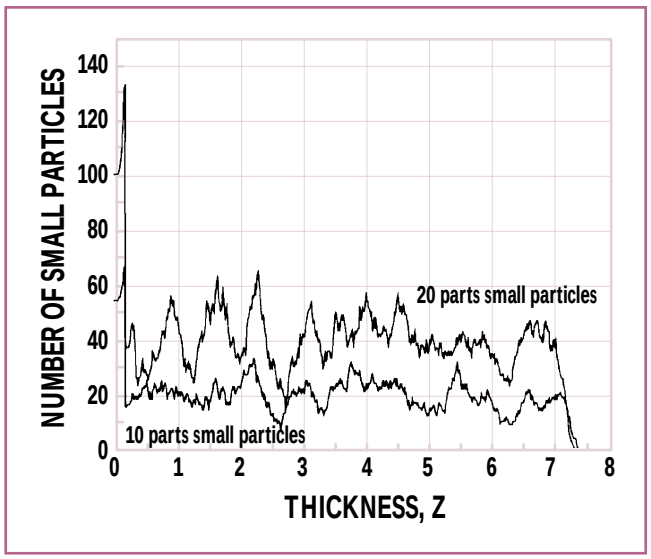

11. Distribution of small particles in the z-direction for different volume fractions for a diameter ratio of 2.5

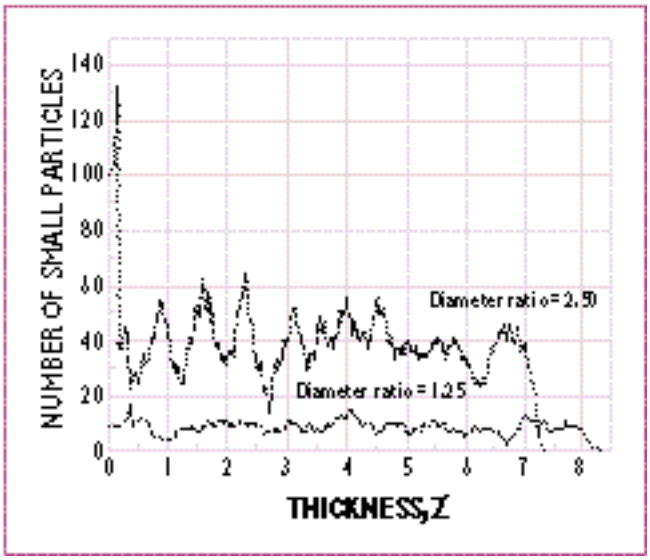

12. Distribution of small particles in the z-direction calculated for different diameter ratios

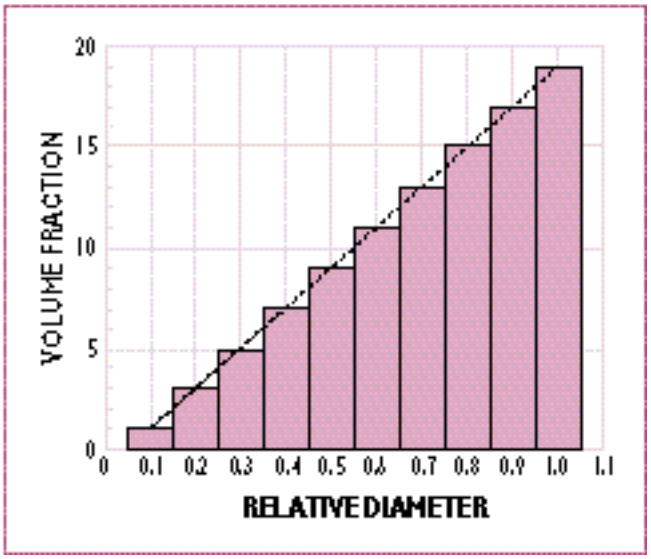

13. Idealized continuous particle size distribution. Positively skewed triangle-shaped particle size distribution (14).

the triangle *IKLM*. As long as the center of the particle that has been placed—particle 4—is in this triangle or on the one of the edges of the triangle, the particle does not roll off.

Periodic boundary conditions

The influence of spheres near the edge of the volume is reflected on the opposite side of the volume by temporarily "moving" particles. This reduces the edge effects, the total number of required particles, and the computation time needed. **Figure 5** shows the periodic boundary conditions applied to the model when a particle is being placed near the right boundary. Particles in the left section of the structure are temporarily moved one cell length. During the placement, the particle moving downward "sees" the particles underneath it even if it rolls out of the unit cell. Consequently, the effect of the particle in the left side of the volume is reflected on the right. After the placement is completed, the particles that have been temporarily positioned on the right are moved back to their original positions. The logic is the same for other boundaries: left, front, and back. If the placed particle ends up outside the cell, it is moved back with all of the other particles.

Calculation of properties from positions

Once the final positions of the particles are determined, a number of small computer codes are written to extract information with regard to porosity, roughness, and pore radius. To calculate porosity and roughness, the top particles need to be identified. These are found by searching small areas and determin-

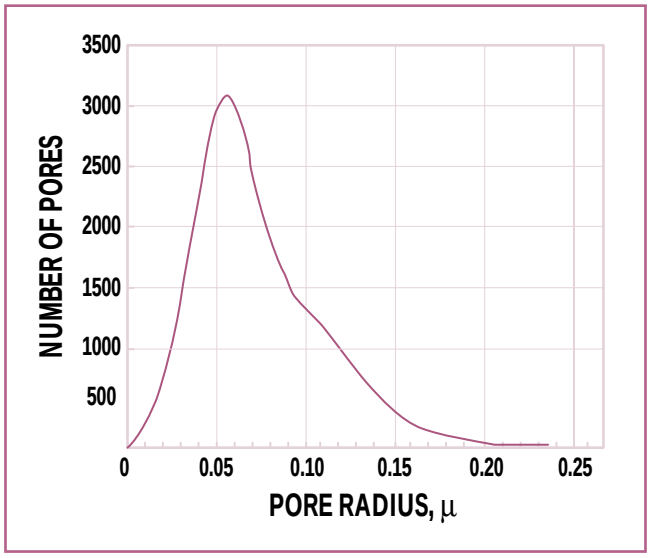

14. Pore radius distribution for conditions as in Fig. 13

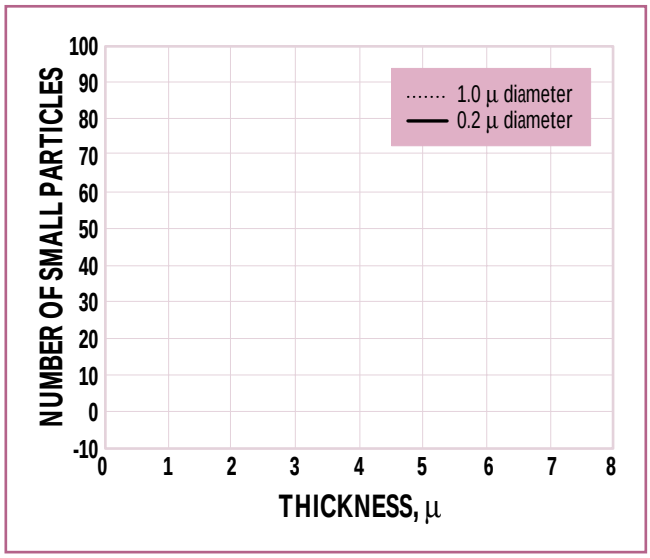

15. Particle size distribution in thickness direction for 0.2- and 1.0-μ size particles

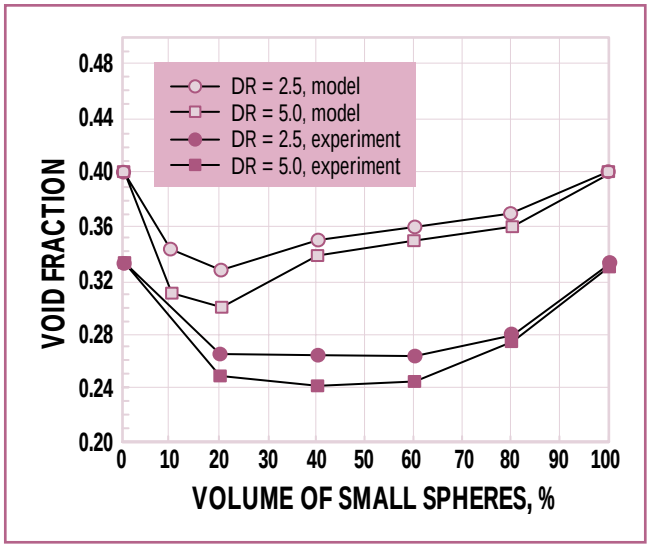

16. Void fraction values are shown as a function of percent volume of small spheres with diameter ratios of 2.5 and 5.0. DR stands for diameter ratio. The filled points are experiments by Alince and LePoutre (21) for polystyrene spheres.

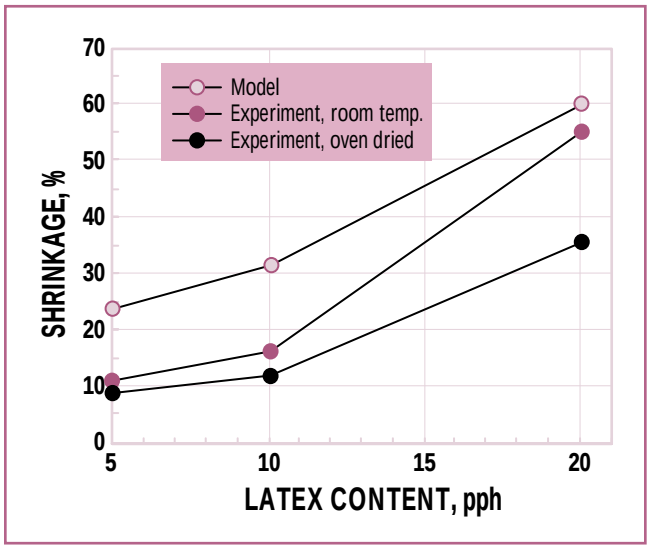

17. Shrinkage is shown as a function of latex content. Dry coat weight is 10 g/m^2, application solid is 60% by weight. $CaCO_3$ coatings. Experiments by Stanislawska and LePoutre (33).

ing the highest particle in each region. Once the top particles are identified, the average height determines the top layer height and the standard deviation of these heights determines the roughness.

To calculate the pore radius distribution, the program checks each group of touching particles. For every four particles touching, there is a pore formed. The volume and shape of that pore is now known in detail. For the purposes of this work, the volume of the pore is calculated based on geometry; details are found in Eksi *(26)*. The volume is converted to a pore radius assuming the pore is a sphere.

The distribution of particles of different size classes inside a structure is calculated by counting the number of particles intersecting horizontal planes. This calculation is repeated for many different horizontal planes. For example, a 1-μ radius sphere with a vertical position of five microns would be counted for all horizontal planes with elevations of 4–6 μ. When this is done for each size class, a complete picture of the location of spheres of different sizes is obtained.

MODEL RESULTS AND DISCUSSION

This section includes the results of uni-modal, bi-modal and poly-modal

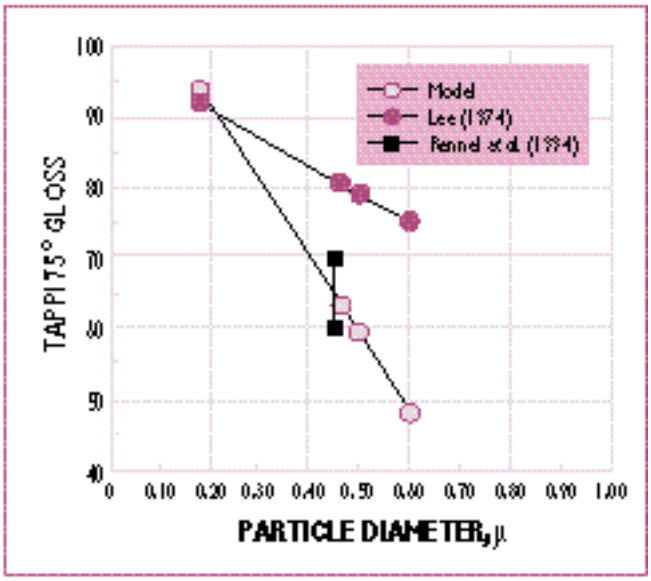

18. Gloss for different polystyrene particle diameters, comparing model results and experiments (31, 34).

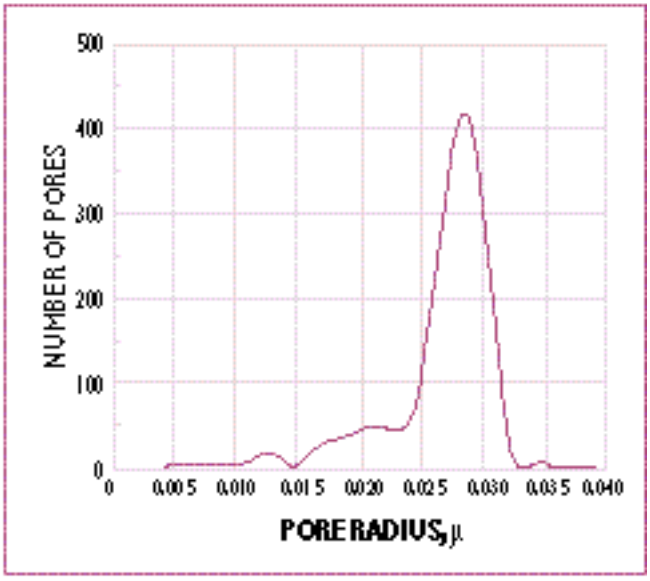

19. Pore radius distribution. 0.1-μ diameter particles.

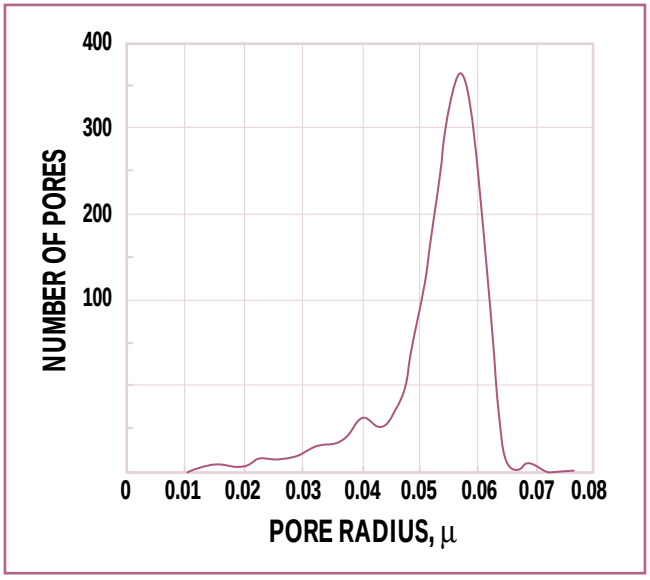

20. Pore radius distribution. 0.2-μ diameter particles.

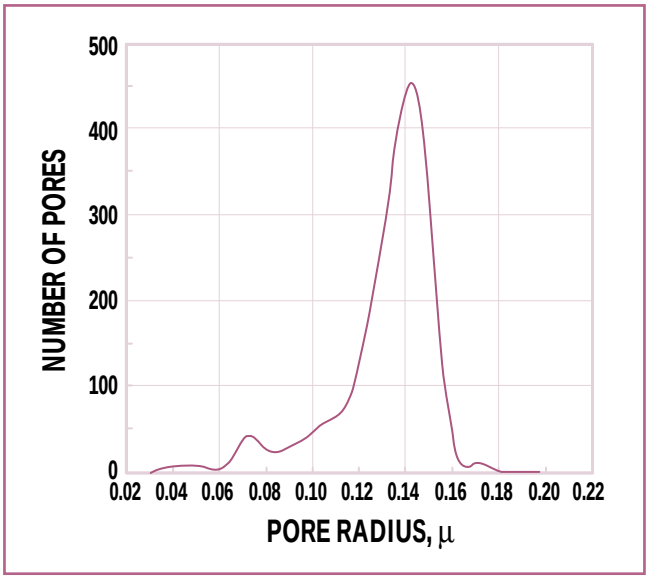

21. Pore radius distribution. 0.5-μ diameter particles.

spherical particles. The intent here is to give detailed results of model systems. After this, comparisons with experiments are made.

Uni-modal particles

The packing of 0.5-μ diameter spheres is discussed. However, all the results scale to any dimension. Void fraction is calculated by finding the average height of the top layer of particles. This height of the top layer, along with the volume of particles and the unit cell dimensions, is used to calculate the void volume. **Figure 6** shows void fraction values as a function of structure thickness. The thickness of the structure is changing from 0.5 (1 layer, 1 diameter thick) to 50.0 μ (100 layers, 100 diameters thick). The highest void fraction value is 0.54, when one layer of particles has been placed. As expected, boundaries disrupt the efficient packing of spheres. The porosity value reaches its constant value of around 0.4, after 5.0-μ thickness, which represents 10 layers of particles. This value compares well with experimental random packing of monosized spheres which are in the range of 0.359 to 0.43 *(10–14)*, and is in excellent agreement with Scott's data *(11)*, 0.399, and Rutger's data *(13)*, 0.404. The result also compares well to other theoretical studies which give results in the range of 0.36 to 0.65 *(3)*.

Surface roughness of a structure is taken as the standard deviation of the height of the top layer of particles. Roughness results found for increasing thicknesses of a structure

are shown in **Fig. 7** for the same structures whose void fraction values are discussed in Fig. 6. As the thickness increases, roughness first increases, and then stays constant after 5-μ thickness, which represents 10 layers of particles. Roughness values start from 0.0 because the base is assumed to be flat. Roughness values calculated in the model are linearly scalable with the particle diameter used.

Bi-modal particles

Figure 8 shows the porosities calculated for binary sphere mixtures as a function of percent volume of small spheres. Diameter ratios of 1.25, 1.7, 2.5, and 5.0 have been used with wet coating thicknesses of 10.0 μ solid content of 50% by volume, and large particle radius of 0.25 μ. As expected, mixing big spheres with small spheres produces a significant change in porosity. For the greater diameter ratio, the variation in porosity is greater. The curves first go through a minimum at a volume of small spheres at 20%. Although the exact percent volume of spheres where the minimum is for each diameter ratio has not been calculated, the value, 20%, compares well with the values reported, which range from 20% to 27% for different diameter ratios *(7, 12, 15, 21, 22)*. This is attributed to the small particles filling the voids between the big particles until the voids are filled by small particles. The location of the minimum depends on the diameter ratio used. The reported locations of this minimum value *(7, 12, 21)* are different from each other. This is because of the different packing density of monosized particles obtained. The maximum reduction in void fraction for 5.0 diameter ratio and 20% volume of small spheres shown in Fig. 8 is 0.10, 50% volume of small spheres. This is not far from the values reported, which are between 0.065, 33% volume of small spheres, and 0.12, 52% volume of small spheres.

Roughness of binary mixtures is calculated for the mixtures whose void fractions are shown in **Fig. 9**. Diameter ratio is again a parameter. Roughness is equal to the value obtained with the 0.5-μ diameter spheres when there are no small particles in the mixture. When the structure is filled with 100% small particles, the result reaches the value of small particles. The increase in percent volume of small particles causes an increase in surface roughness. This unexpected result must be a result of not considering particle sizes when they are placed randomly. There is a significant chance that a few big particles are placed last. This is like placing a big particle on a flat surface: the roughness is close to the particle radius. In a real coating layer, surface tension forces would keep big particles away from the top surface. This feature could be included in the calculations excluding the initial z values to be one radius from the wet thickness. A significant decrease in roughness is shown only when the volume of the small particles is greater than 80%. This result is because small particles fill most of the volume and the effect of big particles is small. As discussed above, this result may be caused by a few big particles placed last.

Average pore radius results calculated for the cell with particles having a diameter ratio of 1.7 and 2.5 in it are shown in **Fig. 10**. As expected, average pore radius decreases as the volume of small particles increases. The increase in diameter ratio of the large to small particles causes a decrease in pore radius.

Figure 11 shows the distribution of small particles along the thickness of a structure built with particles having a diameter ratio of 2.5 with the same parameters as listed in Fig. 8. The distribution of small particles is shown when their percent volume is 10 and 20. For both cases, small particles that fill the first layers and curves show the same behavior. The total number of small particles for 20% volume is larger than that for 10% volume, but if the results were normalized, they would give similar values. However the influence of the boundary can be seen in the structure formed with 20% by volume small spheres: the low points which occur around 0.5, 1.25, 2, and 2.75 seem to reflect layers of big particles. As the particles fill up the structure from one direction, big particles fill up a layer while the small particles fill in the holes in the layer below. This effect gets smaller as the layers become disorganized far from the lower boundary.

Figure 12 shows the comparison of the distribution of small particles for different diameter ratios, 1.25 and 2.5. For the smaller diameter ratio, small particles do not fill in the first layer. This is because small particles are almost as big as the large particles.

Poly-modal particles

Figure 13 shows the particle size distribution used *(14)* in the calculations reported in this section.

Figure 14 shows the pore radius results calculated. The distribution is broader then in the monosized case as expected. The peak value at a pore radius of 0.05 is what would be expected for a 0.15-μ diameter particle, even though there is a significant population of larger particles: the small particles are good at filling in the large pores.

Figure 15 shows the particle size distribution calculated for the particles that have a diameter of 1.0 and 0.2 μ. The small particles are heavily populated at the lower positions. At the top layer, small particles are absent because of the downward (dewatering) placement technique. These results may have important implications for TiO_2 and latex distribution. Again the placement technique does not discriminate with regard to particle size The influence

Void fraction	Diameter, μ
Rennell *et al. (31)*	
0.30	0.45
Alince and LePoutre *(32)*	
0.328	0.1
0.33	0.2
0.329	0.31
0.319	0.37
0.331	0.50
0.35	1.01

I. Void fraction of polystyrene pigment coatings

Particle diameter, μm	Experimental pore radius, μm	Model peak value, μm
0.1	0.03	0.028
0.2	0.055	0.057
0.5	0.15	0.144

***II. Pore radius results for different particle diameters* (32).**

of surface tension forces to keep particles away from the top layer is not taken into account here, but this effect could be included; this effect would produce an increase in small particles at the top instead of the depletion as in Fig. 15.

COMPARISON AND DISCUSSION

This section includes the comparison of the model results with some experimental data reported in the literature. In many cases, this represents the first attempt to compare these experiments with theoretical calculations.

Void fraction

Table I shows the void fraction results based on the experiments performed using monosized polystyrene particles. The coating suspensions were applied on polyester film. The porosities were determined by an oil absorption technique, from the amount of oil held in the voids of the coating after full impregnation followed by removal of the excess oil by wiping *(30)*. The experimental results for these uniform spheres show a very high particle packing density, much higher than random packing. The minimum void fraction for ordered packed spheres is 0.2595 for rhombohedral packing *(1)*. The experimental results of Rennell *et al. (31)* give a void volume of 0.30. These results show that either the particles are ordering through electrostatic forces or surface tension forces are compressing the structure. In addition, the experiments may not be able to see all of the voids, especially near the mylar film surface. The compression or ordering could be included in the model in the future. The model's current packing technique only gives random packing results of 0.4, independent of particle size. The data in Table I average to around 0.33. The difference between the model and the experiments seems to be nearly constant at a 0.33/0.4 ratio.

Figure 16 shows the void fraction values calculated as a function of percent volume of spheres in a binary mixture. Dark points show the experiment values based on the coatings prepared from polystyrene latex particles *(21)*. Diameter of the large particles is 0.5 μ. Solids content is 50% by volume. Although experiment values are lower than the model results, behavior of the curves and reduction in void fraction with increasing small particle percentage are similar. If the void volume of uniform sized particles is adjusted by the ratio of 0.33/0.4, then all of the data points are well predicted as the model.

Shrinkage

Shrinkage results calculated for $CaCO_3$ coatings containing 5, 10 and 20 pph latex binder are shown in **Fig. 17**. Open points are the model results. Dark points show the experiment results *(33)*. Dry coat weight is 10 g/m^2. Solid content is 60% by weight. $CaCO_3$ particles have a rhombic shape. Equivalent spherical diameter of the $CaCO_3$ particles is 1.4μ. Latex particles have a diameter of 0.15 μ. In the experiments, coating suspensions were applied on polyester film. Shrinkage is defined as the percent change in void volume between FCC and the final dry structure. Shrinkage is shown for two different drying conditions, dried at room temperature and in the oven. $CaCO_3$ coatings are chosen because of the rhombic shape of $CaCO_3$ particles even though there is a large particle size distribution.

The higher the latex content, the higher the shrinkage and the higher the roughening of the final structure; this trend agrees with common experimental experience and the literature *(34)*. The shrinkage results calculated for $CaCO_3$ coatings are higher than the experiment results. In the model, it is assumed that all $CaCO_3$ particles have a uniform diameter of 1.4 μ. However, the particles used in experiments are polydispersed. This would cause a low void volume and less ability for shrinkage. Again, surface tension compressive forces should give more shrinkage in the experiments compared to the model.

Gloss

Gloss of the coatings has been found by using the relationship between the surface roughness and gloss *(34, 35)*. Gate *et al. (36)* and Lee *(34)* showed that TAPPI 75° gloss of coat-

KEYWORDS
Adhesives, bibliographies, binders, coatings, coloring materials, consolidation, gloss, mathematical models, microstructure, models, optical properties, particle size distribution, pigment, roughness, separation, surface properties, surface structure, water removal.

ings is only dependent upon their refractive index and surface roughness. Because almost all paper coating materials have similar refractive indices, the TAPPI 75° gloss of paper coatings is mainly dependent upon their surface roughness, regardless of materials used. The relation between TAPPI 75° gloss and surface roughness is given in the literature *(34, 35)*. In the model here, the calculated surface roughness is converted to the gloss given for this literature relationship.

Figure 18 shows the gloss values as a function of particle diameter. Roughness values have been calculated for uniform particles having different diameters, and gloss values have been read from the plot showing the relationship between gloss and roughness *(34, 35)*. While the open symbols represent the model results, dark symbols represent the experiment results *(35)*. Experiments are based on coatings prepared from polystyrene particles. Polyester film substrate has been used in the experiments. Although gloss values found are lower than the experiment values for the experiments by Lee, behaviors are similar. The recent results by Rennel *et al. (31)*, however, are in excellent agreement with the model predictions. The large experimental gloss values of Lee may be a result of surface tension forces flattening out the top surface. This effect is not included in the model at present, but could be included in future work.

Pore radius

Figures 19–21 show the pore radius distribution calculated for 0.1μ, 0.2μ, and 0.5μ diameter particles. Details of the pore radius calculation are in Eksi *(26)*. Experimental results based on the coatings prepared from polystyrene latex particles *(32)* are reported in **Table II.** Pore radii have been calculated from void volume and surface area measurements. Pore radius results calculated from the model are in a very good agreement with the experiment results reported. The peak values match the values reported in Table II within 1.2%. The advantage of the model compared with the experiments is that now a detailed description of the pore space is known, including the characteristics of the surface pores. The pore space characteristics of the top layer compared to the bulk are now known. The structure generated here could aid in the calculation of ink setting on a porous coating layer.

CONCLUSIONS

A three-dimensional particle packing model has been developed to characterize coating structure development during consolidation. This model is the first attempt, to our knowledge, to mathematically describe the consolidation stage based on the physical situation. Particles are placed into a unit cell to simulate the dewatering event. The model predicts the physical arrangement of spherical unimodal, bi-modal and poly-modal particles. Periodic boundary conditions allowed a reduced number of particles to obtain statistically significant results.

From the knowledge of the physical positions of all particles in a unit cell, porosity, roughness, shrinkage, distribution of different sized particles, average pore radius and pore radius distribution have been calculated. The porosity values obtained for monosized and bimodal spheres are in good agreement with experiments, especially if a factor of 3/4 is used.

Particle size distributions of large and small particles in a mixture of bimodal and poly-modal have been calculated. The small particles are heavily populated at the lower positions because of dewatering placement technique, which may have important implication for TiO_2 and latex distribution. Distribution of large particles is steady along the thickness of the structure.

The model predicts that shrinkage and roughening increases with latex content as most experimental results indicate. The shrinkage results calculated for $CaCO_3$ coatings are higher than the experiment results. However, particles used in experiments are polydispersed which cause a low void volume and less ability for shrinkage. Gloss of the coatings is found from the surface roughness; gloss values follow experimental trends as particle size changes. Pore size distribution calculations compare well with the values reported based on the experiments performed with polystyrene latex particles. The model gives information with regard to the details of the pore structure. Porosity and gloss results indicate that surface tension compressive forces may be important in determining the final structure. **TJ**

Eksi is a graduate student and Bousfield is associate professor, Paper Surface Science Program, Dept. of Chem. Eng., University of Maine, Orono, ME 04469-5737.

Received for review Jan. 16, 1996.
Accepted March 19, 1996.
Presented at the TAPPI 1996 Coating Conference.

LITERATURE CITED

1. Graton, L. C. and Fraser, J. H., *J. Geology* 43(8): 785(1935).
2. Cumberland, D. J. and Crawford, R. J., *The Packing of Particles*, Elsevier Science, Amsterdam, The Netherlands. 1987.
3. German, M. R, *Particle Packing Characteristics*, Metal Powder Industries Federation, Princeton, NJ, 1989.
4. Kausch, H. H., Fesko, D. G., and Tschoegl, N. W., *J. of Colloid and Interface Sci.* 37: 603(1971).
5. Vissher, M. W. and Bolsterli, M., *Nature* 239: 504(1972).
6. Matheson, A. J., *J. Phys. C:Solid State Phys.* 7: 2569(1974).
7. Dodds, J. A., *J. Coll. Int. Sci.* 77(2): 317(1980).
8. Davis, L. I. and Carter, R. G., *J. Appl. Phys.* 67(2): 1022(1990).
9. Temperley, J., Westwood, M. J., Hornby, M. R., *et al.*, *J. Coatings Technol.* 64(809): 33(1992).
10. Brown, R. L. and Hawskley, P.G.W., *Nature* 156: 421(1945).
11. Scott, G. D., *Nature* 188: 908(1960).
12. McGeary, R. K., *J. American Ceramic Soc.* 44: 513(1961).
13. Rutgers, R., *Nature* 193: 465(1962).
14. Lee, D. I., *J. Paint Technol.* 42: 579(1970).
15. Van Gilder, R.L., Lee, D. I., Purfeerst, R., *et al.*, *TAPPI 1983 Coating Conference Proceedings*, TAPPI PRESS, Atlanta, p. 123; *TAPPI J.* 66(11): 49(1983).
16. Yerazinus, S., Bartlett, J. W., and Nissan, A. H., *Packing of Nature* 195: 33(1962).
17. Yerazinus, S., Cornell, S. W., and Wintner, B., *Nature* 207: 835(1965).
18. Hagemeyer, R. W., *TAPPI* 43(3): 277(1960).
19. Hagemeyer, R. W., *TAPPI* 47(2): 74(1964).
20. Hagemeyer, R. W., *TAPPI* 47(10): 595(1964).
21. Alince, B. and LePoutre, P., *TAPPI J.* 66(11): 57(1983).
22. Leskinen, A. M., *TAPPI J.* 70(12): 101(1987).
23. Lindhjem, E. C., *TAPPI 1991 Coating Conference Proceedings*, TAPPI PRESS, Atlanta, p. 13.
24. Hoshino, F., Fukaya, S., and Yanagihara T., "Study on Sheet Gloss Development by Addition of Polystyrene Latex Particles," *1993 Advanced Coating Fundamentals*, TAPPI PRESS, Atlanta, p. 81.
25. Watanabe, J. and LePoutre, P., *J. Appl. Poly. Sci.* 27: 4207(1982).
26. Eksi, G., "Modeling of coated structure development," M.S. thesis, University of Maine, Orono, ME, 1995.
27. Toivakka M., Eklund, D., and Bousfield, D. W., *TAPPI 1991 Forest Products Symposium Notes*, TAPPI PRESS, Atlanta, p. 158.
28. Toivakka, M., Eklund, D., and Bousfield, D. W., *TAPPI 1992 Coating Conference Proceedings*, TAPPI PRESS, Atlanta, p. 403.
29. Press, H. W., Teukolsky, A. S., Vetterling, T. W., *et al.*, *Numerical Recipes in Fortran, The Art of Scientific Computing*, 2nd edn., Cambridge University Press, 1992, p. 270.
30. LePoutre, P. and Rezanowich, A., *Tappi* 60(11): 86(1977).
31. Rennel, C., Eriksson, U., and Rigdahl, M., *Nordic Pulp and Paper Research J.* 9(4): 254(1994).
32. Alince, B. and LePoutre, P., *J. Coll. Int. Sci.* 76: 182(1980).
33. Stanislawska, A. and LePoutre, P., *TAPPI 1995 Coating Conference Proceedings*, TAPPI PRESS, Atlanta, p.67.
34. Lee, D., *TAPPI 1974 Coating Conference Preprints*, TAPPI PRESS, Atlanta, p. 97.
35. Lee, D.I. and Hendershot, E. R., *TAPPI 1986 Coating Conference Proceedings*, TAPPI PRESS, Atlanta, p. 31.
36. Gate, L., Windle, W., and Hine, M., *TAPPI* 56(3): 61(1973).

We want to thank the members of the University of Maine Paper Surface Science Program for their financial support and suggestions. We thank Pierre LePoutre for many helpful discussions. Thanks to the Turkish government for Eksi's scholarship.